The infrared spectrum of the ν_2 fundamental band of the H_3^+ molecular ion

J. K. G. WATSON, S. C. FOSTER, A. R. W. MCKELLAR, P. BERNATH,[1] AND T. AMANO
Herzberg Institute of Astrophysics, National Research Council of Canada, Ottawa, Ont., Canada K1A 0R6

AND

F. S. PAN, M. W. CROFTON, R. S. ALTMAN, AND T. OKA[2]
Department of Chemistry and Department of Astronomy and Astrophysics, The University of Chicago, Chicago, IL 60637 U.S.A.

Received June 8, 1984

The observation and analysis of 46 lines of the infrared ν_2 band of the H_3^+ molecular ion are described. The data include 16 new observations as well as the 30 previously published lines. The spectra are observed in absorption in a hydrogen discharge using tunable monochromatic sources, either a laser difference-frequency system or a diode laser. Two modulation techniques, either discharge amplitude modulation or Doppler velocity modulation, are used to increase the sensitivity. Ground state combination differences between the observed lines are in good agreement with *ab initio* calculations, and scaled *ab initio* rotational term values are used to relate the different K-energy stacks. Padé-type expressions are found useful in representing the line frequencies, and 44 lines are fitted by 23 parameters with a standard deviation of 0.014 cm^{-1}. The two lines omitted appear to be perturbed by a rovibrational interaction between the ν_2 and ν_1 states that should become more important for higher values of J.

On décrit l'observation et l'analyse de 46 raies de la bande infrarouge ν_2 de l'ion moléculaire H_3^+. Les données incluent 16 nouvelles observations en plus de 30 raies déjà connues. Les spectres ont été observés en absorption dans une décharge dans l'hydrogène, en utilisant une source monochromatique à fréquence variable, soit un système laser à fréquence différentielle ou un laser à diode. Deux techniques de modulations, modulation de l'amplitude de la décharge ou modulation Doppler de la vitesse, ont été utilisées pour accroître la sensibilité. Les différences de combinaisons de l'état fondamental entre les raies observées sont en bon accord avec les calculs *ab initio*, et les valeurs *ab initio* des termes rotationnelles sont utilisées, avec un facteur d'échelle, pour relier les différents groupes d'énergie K. Des expressions de type Padé se sont avérées utiles pour représenter les fréquences des raies, et 44 raies ont été ajustées au moyen de 23 paramètres, avec un écart type de 0,014 cm^{-1}. Les deux raies laissées de côté semblent être perturbées par une interaction rovibrationnelle entre les états ν_2 et ν_1 qui devrait devenir plus importante pour les valeurs plus élevées de J.

[Traduit par le journal]

Can. J. Phys. **62**, 1875 (1984)

1. Introduction

The H_3^+ molecular ion is a fundamental chemical species that has played an important role in many areas of science since its discovery in 1912 by Thomson (1). The high proton affinity (4.4 eV) of H_2 means that H_3^+ is a well-bound, physically stable system, and it is produced efficiently through the 1.7-eV-exothermic, ion–molecule reaction (2)

$$[1] \quad H_2 + H_2^+ \rightarrow H_3^+ + H$$

which has a large Langevin cross section (3, 4). Thus, H_3^+ is a major cation in hydrogen discharges (5, 6) and is an important ingredient in ion–molecule reaction schemes involving hydrogen. In particular, for molecule formation in dense interstellar clouds (7–11), the production of H_3^+ initiated by cosmic ray ionization of H_2, and the subsequent protonation of neutral species X through the reaction

$$[2] \quad H_3^+ + X \rightarrow HX^+ + H_2$$

is so universal that this reaction scheme is often called H_3^+ chemistry.

As the simplest two-electron polyatomic system, the H_3^+ ion is also important as a testing ground for *ab initio* molecular theory. There have been over 40 theoretical papers on this ion, ranging from the pioneering work of Hirschfelder (12), showing the triangular geometry to be the most stable, through to the recent extensive work of Carney and Porter (13–16), predicting the structure and vibrational frequencies with high accuracy. These and many other studies of H_3^+ have been reviewed recently from both an experimental (17) and a theoretical (18) viewpoint, and the reader is referred to these reviews for more details. Among the developments subsequent to these reviews may be mentioned the detailed study by Carrington and Kennedy (19) of

[1]Present address: Department of Chemistry, University of Arizona, Tucson, AZ 85721 U.S.A.

[2]Previous address: Herzberg Institute of Astrophysics, National Research Council of Canada, Ottawa, Ont., Canada K1A 0R6.

the extensive near-dissociation spectrum; the new *ab initio* calculations of vibration (20) and vibration–rotation (21) energies, both of which are in general agreement with the earlier work of Carney and Porter (13–16); and the recent observation and assignment of lines of the ν_1 bands of H_2D^+ by Amano and Watson (22) and HD_2^+ by Lubic and Amano (23). Lines of the ν_2 and ν_3 bands of H_2D^+ and HD_2^+ and of the ν_2 band of D_3^+ have also been observed in our laboratories, and the analysis of them is in progress.

The importance of the spectroscopic study of the H_3^+ ion has long been advocated by Herzberg (24). He pointed out that since *ab initio* theory predicts no stable, excited, singlet electronic states, the degenerate ν_2 band in the infrared is probably the easiest spectrum to observe. Eventually, in 1980, 15 spectral lines belonging to this band were observed by Oka (25). The observation was based on two recently developed techniques, namely the positive column glow discharge introduced for microwave spectroscopy by Woods (26), and the difference-frequency laser system of Pine (27), which provides a widely tunable, monochromatic, infrared radiation source. Subsequently (28), an additional 15 lines were measured by Oka and Bernath, based on predictions from the previous lines by Watson. More details and episodes in the progress of this project may be found in the review on H_3^+ by Oka (17) and one on hydrogenic species by Herzberg (29).

In the present paper we collect together the latest measurements of altogether 46 lines of the ν_2 band of H_3^+, and discuss the overall analysis and fitting of the data. The new lines added since ref. 28 are mostly lower frequency or weaker lines. The measurements of the former were made possible by two techniques, either by using diode lasers or by extending the lower frequency limit of the difference-frequency system by using Ar^+ lines other than 5145 or 4880 Å. Observations of the weaker lines depended on improvements in sensitivity resulting from either discharge amplitude modulation (30, 22, 23) or Doppler modulation (31).

2. Experimental

These infrared spectral lines of H_3^+ have again been observed in absorption in discharges through hydrogen gas, employing as tunable infrared sources either (a) the difference frequency of two visible lasers or (b) the direct output of semiconductor diode lasers.

2a. Measurements with the difference-frequency laser system

The difference-frequency laser system developed by Pine (27) provides a nearly ideal tunable source for the spectroscopy of ν_2 of H_3^+. By mixing radiation from an Ar^+ laser (ν_A) and a dye laser (ν_D) in a temperature-controlled $LiNbO_3$ crystal, we obtain monochromatic infrared radiation with a power of the order of 10 μW, whose frequency ($\nu_A - \nu_D$) is tunable over the range 2250–4400 cm^{-1}. This tuning range covers the central- and high-frequency portion of the ν_2 band of H_3^+, whose band origin is at 2521 cm^{-1}.

A schematic diagram of the apparatus is shown in Fig. 1. This is the original version of the apparatus, used in refs. 25 and 28; see also ref. 32. A Spectra Physics 580 dye laser, or later a Coherent 699 ring laser, pumped by an Ar^+ laser generated visible radiation in the red to yellow region of the spectrum. This radiation was mixed in the $LiNbO_3$ crystal with either 5145 or 4880 Å, or later 4965 or 5017 Å, radiation from a single-mode Ar^+ laser. For frequency modulation of the radiation, the frequency of the single-mode Ar^+ laser was modulated with an amplitude of about 400 MHz and a frequency of 2.5 kHz by modulation of the laser cavity length. An etalon mounted on a piezoelectric element inserted in the laser cavity was modulated synchronously to maintain a constant level of power output. The multiple reflection, direct current (dc) discharge tube was 2 m long with a diameter of 2 cm and was cooled with liquid nitrogen, as was done by Woods and Dixon (33). The discharge tube was sealed with two CaF_2 Brewster angle windows and placed inside a multiple reflection mirror system. An absorption path of 32 m was normally used (25), while for higher-J transitions (28), water cooling replaced the liquid nitrogen. Further details of these earlier experiments are described in ref. 32.

More recently, this Ottawa apparatus has been used with discharge amplitude (30) rather than frequency modulation. This technique was also applied to the ν_1 lines of H_2D^+ (22) and HD_2^+ (23), and further details can be obtained from ref. 22. The higher sensitivity achieved made it possible to observe several of the weaker R-branch lines of H_3^+.

In the later version of the apparatus built in Chicago, a liquid-nitrogen cooled, 1-m alternating current (ac) discharge cell with a diameter of 1.2 cm was used. The Doppler modulation method developed by Gudeman *et al.* (31) eliminated the need for frequency modulation and also increased the sensitivity by about an order of magnitude. A unidirectional multipassing system was used, normally with six passes so that the overall absorption pathlength was 6 m. A noise subtraction method (34) further increased the sensitivity. An example of an observed line is presented in Fig. 2*a*. This line is approximately 10 times weaker than the strongest lines shown in ref. 25. The discharge amplitude modulation method has also been used with this apparatus, allowing absorption paths comparable to the original dc discharge pathlengths (25).

The wavenumbers of the H_3^+ lines were measured by interpolation between absorption lines of reference

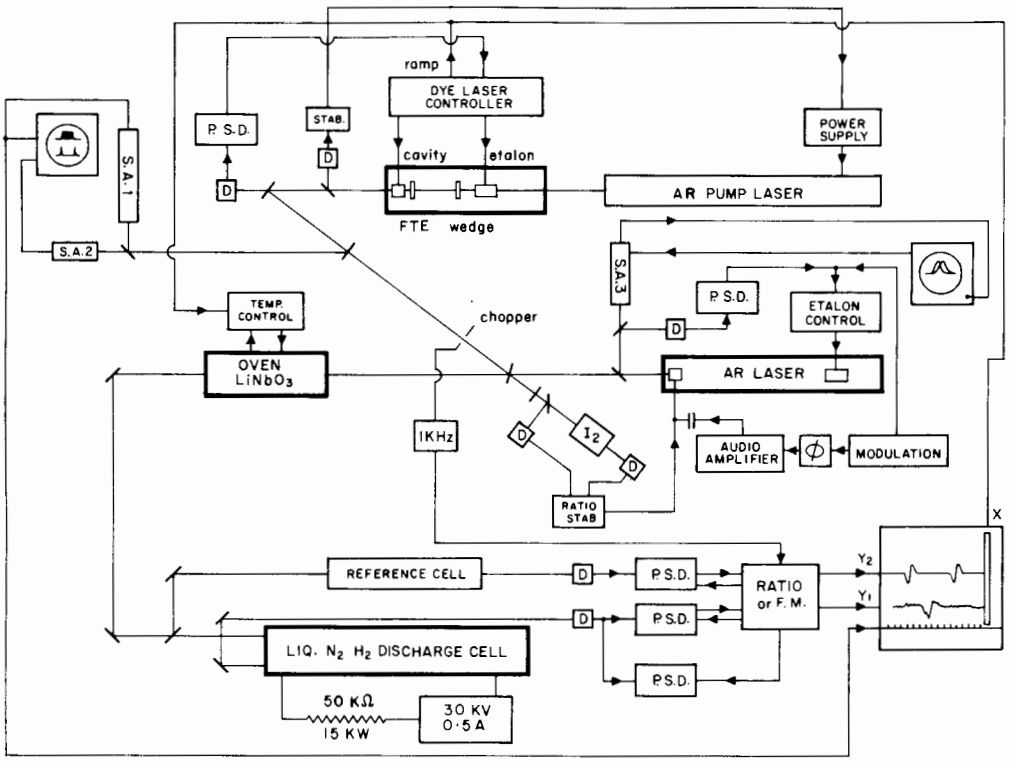

FIG. 1. Schematic diagram of the difference-frequency laser apparatus used for the original detection of the spectrum of H_3^+. Subsequent modifications of the apparatus are described in Sect. 2.

gases. Lines of N_2O, H_2CO, and C_2H_4, and CO_2 and PH_3, were used in the higher- and lower-wavenumber portions of the H_3^+ band, respectively.

2b. Measurements with tunable diode lasers

Measurements of the $P^+(3)$, $P^+(4)$, and $Q^-(4)$ groups of lines were made in Ottawa with a tunable diode laser spectrometer and an absorption cell similar to that of Van den Heuvel and Dymanus (35), consisting of a copper hollow cathode (length 70 cm, diameter 5 cm) mounted in a 1-m pyrex tube fitted with multiple reflection mirrors (36). The cathode was cooled with liquid nitrogen for the $P^+(3)$ and $Q^-(4)$ observations, and with water for $P^+(4)$, and 16 traversals gave an effective path length of 11.2 m in the discharge region. The discharge amplitude modulation method (30, 22) was employed by switching the current through the cell on and off with a frequency of about 9 kHz, thereby modulating the H_3^+ concentration. Phase-sensitive amplification of the signal at the modulation frequency gave a true transmission (zeroth derivative) line shape. The discharge current was provided by an 800-W audio amplifier driving a 25:1 step-up transformer. With the resulting ac voltage (ca. 3 kV peak−peak) applied to the cell anode and the cathode grounded, the cell acted as a rectifier, conducting only on the half cycles for which the anode is positive. The peak current was generally about 0.6 A, and the pressure in the cell was 0.2−0.3 Torr of pure H_2 (1 Torr = 133 Pa). The wavenumbers of the H_3^+ lines were measured relative to nearby absorption lines of N_2O and CO_2 with the aid of a temperature-stabilized Ge etalon. An example of one of the diode laser observations is shown in Fig. 2*b*.

3. Assignments and theoretical model

The data set considered here consists of 46 lines of H_3^+, of which 39 were measured with the laser difference system and 11 with the diode laser spectrometer. For the four lines in common, the diode measurements are consistently higher than the laser difference measurements, by 0.007_5 cm^{-1} on average. This discrepancy, which is quite significant in relation to the line width (full Doppler width = 0.015 cm^{-1} at 200 K), is probably due to calibration errors, and contributes to the standard deviation of the combined fit. To minimize its effects, data from a common source are used for all the K components of each J transition. The observed lines and assignments are presented in Table 1. A few additional observed lines may be higher-J transitions of H_3^+, but it is difficult to extrapolate with confidence,

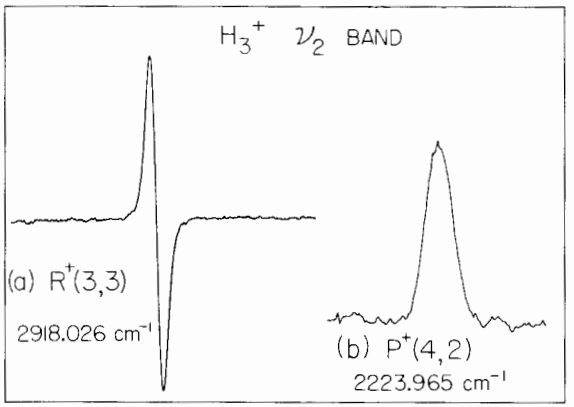

FIG. 2. Recordings of two lines of the ν_2 band of H_3^+. Spectrum (*a*) was obtained with a liquid-nitrogen cooled discharge using the difference-frequency laser system and the Doppler modulation technique. Spectrum (*b*) was obtained with a water-cooled discharge using the diode laser system and the discharge amplitude modulation technique. In both cases, the integration time constant was 1 s. Note that these transitions are one to two orders of magnitude weaker than the strongest lines of the band.

and these lines might also conceivably belong to the triplet–triplet bands of H_2 in this region (37), which have recently been observed in absorption by one of us (T.A.). The assignments of these extra lines are not considered further here.

Initial assignments (25) were made by comparison between the observed lines and a theoretical spectrum calculated from an effective Hamiltonian (38), using parameters derived from the *ab initio* matrix elements of Carney and Porter (13–16). The major change required was an overall shift of about 5 cm^{-1}. Some of the principal constants were adjusted to fit the assigned lines, then more assignments were made based on the new theoretical spectrum, further constants were adjusted, and so on. Little difficulty was experienced in this iterative procedure for low J's, because the lines are in general widely spaced and there is little ambiguity in the assignments. However, the K components of some of the J transitions are more closely spaced, and for them the numbering of the K structure was more difficult, particularly at higher J's on the high-frequency side of the Q-branch, where the $Q^+(J,K)$ patterns of different J's overlap. The effective Hamiltonian converges very slowly, and extrapolations by this method beyond $J = 5$, where the contributions from the H centrifugal terms can be several cm^{-1}, become extremely uncertain.

In an attempt to overcome this extrapolation difficulty, the use of Padé-type expressions (39–42) for the rotational Hamiltonian or term values was investigated. The results from these Padé fits proved to be very encouraging, not only from the point of view of extrapolation, but also because they appeared to provide a better model for the lower J values, where some ambiguities in the K numbering were resolved. For example, the region of $Q^-(4)$ caused some difficulty because two

TABLE 1. Observed lines and assignments in the ν_2 band of H_3^+

J'	G'	U'	J''	K''	$\nu_{obs.}$ (cm^{-1})	Residual (cm^{-1})*
3	4	1	4	4	2217.451	−0.001
3	3	1	4	3	2218.129	0.015
3	2	1	4	2	2223.965	−0.010
3	1	1	4	1	2229.895	−0.007
2	1	1	3	1	2295.577	−0.004
2	2	1	3	2	2295.947	−0.016
2	0	1	3	0	2295.980	0.019
2	3	1	3	3	2298.930	−0.000
1	1	1	2	1	2372.185	−0.002
1	2	1	2	2	2378.869	−0.004
0	1	1	1	1	2457.290	0.011
4	3	−1	4	3	2486.559	−0.007
4	2	−1	4	2	2491.749	0.012
4	1	−1	4	1	2492.541	0.001
3	2	−1	3	2	2503.347	−0.005
3	1	−1	3	1	2508.131	0.004
3	0	−1	3	0	2509.075	−0.012
2	1	−1	2	1	2518.207	−0.001
1	0	−1	1	0	2529.724	0.007
1	1	1	1	1	2545.418	−0.003
2	1	1	2	1	2552.987	−0.006
2	2	1	2	2	2554.664	−0.017
3	3	1	3	3	2561.493	0.014
2	1	−1	1	1	2691.444	0.003
2	0	1	1	0	2725.898	0.014
2	1	1	1	1	2726.219	−0.007
3	2	−1	2	2	2762.068	−0.002
3	1	−1	2	1	2765.547	0.008
3	2	1	2	2	2823.136	−0.006
3	1	1	2	1	2826.113	−0.004
4	3	−1	3	3	2829.923	−0.008
4	1	−1	3	1	2831.340	−0.003
4	2	−1	3	2	2832.197	0.010
5	2	−1	4	2	2891.880	−0.234†
5	4	−1	4	4	2894.488	0.000
5	3	−1	4	3	2894.610	−0.008
4	3	1	3	3	2918.026	0.014
4	2	1	3	2	2923.361	0.024
4	1	1	3	1	2928.351	−0.014
4	0	1	3	0	2930.163	−0.004
6	5	−1	5	5	2956.072	0.006
5	4	1	4	4	3008.115	−0.015
7	6	−1	6	6	3014.358	−0.001
5	3	1	4	3	3015.240	0.003
5	2	1	4	2	3024.547	−0.387†
5	1	1	4	1	3029.823	0.002

*Residual (obs. − calc.) in the least squares fit (Sect. 4).
†Not included in least squares fit.

extra lines (possibly due to H_2) were observed in this region, and it was not clear which lines belonged to H_3^+ or what their K values were. However, one of the possible assignments was definitely preferred in the Padé fit, and was independently supported by the observed relative intensities.

The most successful Padé form tested so far consisted of a modification of the $V_2 = 1$ term-value expression, [27] of ref. 38, in which the higher-order terms were removed and Padé denominators were introduced in a fairly ad hoc way. The explicit form is

$$[3]\quad T_{vr}(V_1, V_2 = 1, J, G, U, s) = G_v - 2(C\zeta_2)_v + B_v J(J+1) + (C_v - B_v)(G^2+1) + \eta_2^J J(J+1) + \eta_2^K(3G^2+1) + \left\{-D_v^{JJ}J^2(J+1)^2 - D_v^{JK}J(J+1)(G^2+1) - D_v^{KK}(G^4+6G^2+1) + \frac{1}{2}s\delta_{G3}\beta_2(J-1)J(J+1)(J+2)\right\}\Big/\{1 + d_J J(J+1) + d_K G^2\} + U\left\{4Z^2G^2 + \frac{1}{4}Q^2(J-G)(J+G)(J+1-G)(J+1+G)\right\}^{1/2}\Big/\{1 + e_J J(J+1) + e_K G^2\}$$

$$[4]\quad Z = C_v - B_v - (C\zeta_2)_v + \frac{1}{2}\eta_2^J J(J+1) + \frac{1}{2}\eta_2^K(G^2+3) - D_v^{JK}J(J+1) - 2D_v^{KK}(G^2+1) - \frac{1}{12}s\delta_{G3}\beta_2(J-1)J(J+1)(J+2)$$

$$[5]\quad Q = q_2 + 2s\delta_{G3}h_3(J-1)J(J+1)(J+2)$$

Here J and $G = |k - l_2|$ are the usual quantum numbers, the values $U = \pm 1$ distinguish the upper and lower components of the l doubling or l resonance, and $s = \pm 1$ distinguishes the components of the $G = 3$ splitting. For H_3^+, the nuclear spin statistics imply that only the levels with $s = (-1)^{J+1}$ are populated, so that the label s is unnecessary. The special cases $G = 0$, J, or $J + 1$ are treated as described on p. 360 of ref. 38. Apart from the denominator parameters d_J, d_K, e_J, and e_K, the constants in [3]–[5] have their conventional meanings. The $V_2 = 0$ formula, [20] of ref. 38, is modified in an analogous way,

$$[6]\quad T_{vr}(V_1, V_2 = 0, J, G = K, s) = G_v + B_v J(J+1) + (C_v - B_v)K^2 - \{D_v^{JJ}J^2(J+1)^2 + D_v^{JK}J(J+1)K^2 + D_v^{KK}K^4\}/\{1 + d_J J(J+1) + d_K K^2\} + s\delta_{K3}h_3(J-2)(J-1)J(J+1)(J+2)(J+3)$$

From expressions [3] and [6] there are altogether 24 parameters in the line frequencies of the ν_2 band, but the parameter sets C_0, C_2, $C\zeta_2$ and D_0^{KK}, D_2^{KK}, η_2^K are each experimentally inseparable because of the $\Delta G = 0$ selection rule on the allowed transitions. This means that the relative energies of the different G stacks cannot be determined experimentally, and either theoretical relations (38) must be used to constrain the indeterminancies affecting C_v, D_v^{KK}, . . . , or suitable *ab initio* calculated energy levels must be included as data. After some tests, the latter course was adopted here. As an additional constraint, the $K = 3$ splitting constant h_3 of the ground state was assumed to have the same value in the ν_2 state, where it contributes to the l resonance for $G = 3$. Thus, there are a total of 23 adjustable parameters in the final least squares fit.

Other Padé models have been treated, mainly by representing the effective Hamiltonian operator (38) in a Padé form with more parameters than above, and then applying constraints such as [11], [14], or [15] of ref. 38 to the power series expansions of the Padé operator. These models encountered great difficulties because of strong correlations in the least squares fits that tended to produce large increments in the parameters, with the result that some of the denominators could become small for some levels and the energy formulas became nearly singular. Damping of the least squares seemed merely to delay the explosion. Further work on these types of approximations is clearly necessary.

In the particular approximation [3]–[5] used here, the same denominator is used in the Z and Q contributions to the matrix elements. As a result, the eigenvectors are given by [29]–[30] of ref. 38 with expressions [4]–[5] for Z and Q, because the denominators cancel in the normalization, and the line strengths are given by [31] of ref. 38. The calculated relative intensities are particularly useful as additional evidence in assigning closely spaced groups of lines, such as the K components of $P^+(3)$.

TABLE 2. Ground state combination differences of H_3^+ (cm^{-1})

Ground state difference $(J_1'', K'') - (J_2'', K'')$	Upper level (J', G', U')	$\Delta\nu_{obs.}$	$\Delta\nu_{calc.}$*	$\Delta\nu_{calc.}$†
(3, 0) − (1, 0)	(2, 0, 1)	429.918	431.47	429.426
(2, 1) − (1, 1)	(1, 1, 1)	173.233	173.74	173.045
	(2, 1, −1)	173.237		
	(2, 1, 1)	173.232		
(3, 1) − (2, 1)	(2, 1, 1)	257.410	258.40	257.112
	(3, 1, −1)	257.416		
(4, 1) − (3, 1)	(4, 1, −1)	338.799		338.391
(4, 1) − (2, 1)	(3, 1, 1)	596.218‡		595.503
(3, 2) − (2, 2)	(2, 2, 1)	258.717	259.60	258.438
	(3, 2, −1)	258.721		
(4, 2) − (3, 2)	(4, 2, −1)	340.448		340.044
(4, 2) − (2, 2)	(3, 2, 1)	599.171§		598.482
(4, 3) − (3, 3)	(3, 3, 1)	343.364		342.996
	(4, 3, −1)	343.364		

*Reference 15.
†Reference 21.
‡Also 596.212 (mean) from {(4, 1) − (3, 1)} + {(3, 1) − (2, 1)}.
§Also 599.167 (mean) from {(4, 2) − (3, 2)} + {(3, 2) − (2, 2)}.

4. Results

The assignments of the lines are given in Table 1 according to the notation $(J', G, U') - (J, K = G)$. Note that because of the nuclear spin statistics, for $G = 0$ only levels with odd J are allowed in the ground state while only levels with $U' = (-1)^{J'}$ are allowed in the upper state. By taking differences between lines of Table 1 with common upper levels, we obtain the ground state combination differences presented in Table 2. One check of internal consistency comes from combination relations, which are represented in Table 2 by multiple determinations of the same ground state difference. The discrepancies in the combination relations are of the order of 0.005 cm^{-1}, similar to the calibration errors (Sect. 3). Thus, the combination relations are satisfied within experimental error.

Without the observation of forbidden transitions (43), the ground state combination differences obey the rule $\Delta K = 0$. Table 2 shows that for each K value, the relative energies of all the J levels with $J \leq 4$ are known. These are compared with differences of *ab initio* term values from the calculations of Carney (15) and Tennyson and Sutcliffe (21), which are on average 0.34% higher and 0.115% lower, respectively.

The seven independent ground state differences in Table 2 can only be fitted to 0.021 cm^{-1} with a conventional Hamiltonian with the three constants B_0, D_0^{JJ}, and D_0^{JK}. The inclusion of H_0^{JJJ}, H_0^{JJK}, and H_0^{JKK} allows the data to be fitted within experimental error, but there are six parameters for seven data. Nevertheless, the values obtained for the constants are reasonable when compared with values derived either from fitting the *ab initio* term values (15, 21) or from the theoretical formulas (38) using potential constants from the *ab initio* calculations (13−16). Because the ground state is well behaved, these observed ground state differences were included as extra data with a weight of 10 in the least squares fit of the lines of the ν_2 band.

To overcome the indeterminacies in the ν_2 fit produced by the $\Delta G = 0$ selection rule, the constants C_v, D_v^{KK}, ... must be constrained. In the present case we could use either theoretical values for the planarity defects or the fact that the planarity defects are proportional to $(V_2 + 1)$ (38). Both of these methods depend on ignoring higher-order effects, and therefore may be unreliable for this very light molecule. These methods were tried and the resulting K-energy separations of the ground state were compared with the *ab initio* calculations (15, 21). It was concluded that the discrepancies were probably due to errors in the experimental values, and that the most accurate present estimates of the relative K energies are obtained by scaling the *ab initio* ground state energies by a common factor determined from the combination differences. The implicit assumption that the *ab initio* values of B_0 and C_0 are in error by the same factor is probably fairly accurate. The specific procedure chosen was to treat the four $J = K$ ground state levels of Tennyson and Sutcliffe (21) with $J = 1-4$ as additional data, after multiplication by the factor 1.00115. This is sufficient to fix the relative energies of the different K stacks without otherwise forcing agreement with the *ab initio* calculations.

TABLE 3. Vibration–rotation parameters for the ν_2 band of H_3^+ (cm^{-1})

Parameter i*	Value (SD)†	Correlation κ_i‡	*Ab initio*§	*Ab initio*‖
		Ground state		
B_0	43.564570(1553)	163.2	43.668	43.520
C_0	20.605147(2993)	167.7	20.675	20.579
$10^2D_0^{JJ}$	4.17537(1900)	2 248.5	3.72	4.22
$10^2D_0^{JK}$	−7.60626(4096)	3 332.9	−6.70	−7.76
$10^2D_0^{KK}$	3.74107(3683)	1 797.7	3.29	3.85
10^5h_3	−1.056(100)	5.7		−0.9
10^3d_J	1.7325(1529)	348.6		2.0
10^3d_K	−4.1003(4428)	190.4		−4.6
		ν_2 state		
ν_2	2521.30817(925)	18.2	2516	2494.4
B_2	44.225698(3011)	242.1	43.839	
C_2	19.339581(6389)	1 000.8	19.735	
$C\zeta_2$	−18.65110(384)	49.7	−18.516	
$10^2\eta_2^J$	−14.0319(858)	691.4		
$10^2\eta_2^K$	16.7714(1937)	2 659.1		
$10^2D_2^{JJ}$	5.27821(3051)	7 814.5		
$10^2D_2^{JK}$	−10.87796(9077)	36 917.6		
$10^2D_2^{KK}$	6.07921(6385)	12 807.9		
$10^3\beta_2$	−3.1598(363)	3.3		
q_2	−5.37192(254)	33.8	−4.87	
10^5h_3	−1.056(100)	5.7		
10^3d_J	2.0467(1481)	691.2		
10^3d_K	−1.8823(3657)	1010.0		
10^3e_J	4.0396(307)	263.6		
10^3e_K	−7.1747(1467)	1772.6		

*The parameters are defined in the Padé formulas [3]–[6].

†Values are in cm^{-1}, with standard deviations (SD) in units of the last quoted decimal place. The numbers of digits are chosen according to ref. 44 with 'safety factor' $f = 0.1$.

‡Correlations $\kappa_i = (\chi^{-1})_{ii}$, where χ is the matrix of correlation coefficients (see Sect. 4).

§Ground state constants by fitting the $J \leq 3$ term values of ref. 15 to five parameters. Excited state constants from ref. 16.

‖Ground state constants by fitting the $J \leq 4$ term values of ref. 21 to eight parameters. Excited state term value from ref. 21.

The model finally adopted for the energy levels used the Padé formulas presented in Sect. 3. The values of these formulas can become very large if any of the denominators becomes small, as can happen if a least squares iteration overshoots because of the nonlinearity of the equations. Thus it is desirable to introduce the data and parameters in a stepwise way, to avoid large increments in the parameters in any iteration. It is also good policy to monitor the size of the denominators, in case any become dangerously small. For the particular formulas [3] and [6], this problem was not serious and the fits generally converged in three or four iterations. The two lines $R^+(4, 2)$ could not be fitted satisfactorily and were omitted. A possible perturbation of these lines is discussed below. In the final fit, 48 data (44 observed lines and 4 scaled *ab initio* energies) were fitted by 23 parameters with a standard deviation of $\sigma = 0.014\ cm^{-1}$. Although this is still larger than the experimental error, this fit seemed a satisfactory compromise between accuracy of fit and an excessive number of parameters. The residuals in this fit are presented in Table 1 and the final constants in Table 3, which includes a comparison with *ab initio* values.

The correlation of parameter i is indicated in Table 3 by the diagonal element $\kappa_i = (\chi^{-1})_{ii}$ of the inverse of the correlation matrix. This is a measure of the correlation of the parameter i with all the other parameters. Uncorrelated parameters have $\kappa_1 = 1$, whereas a two-parameter problem would have $\kappa_1 = \kappa_2 = 1/(1 - \chi_{12}^2)$. The κ_i parameters give a more compact indication of the

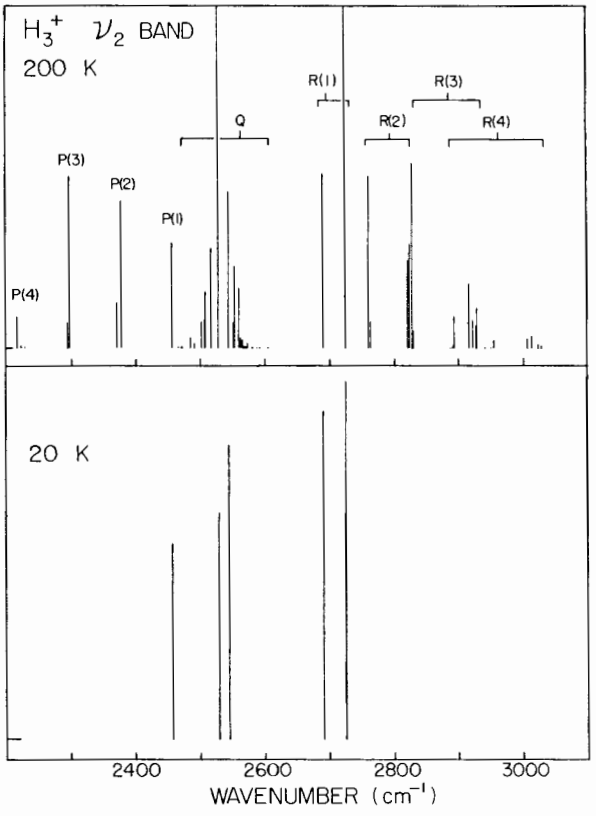

FIG. 3. Calculated spectra of the ν_2 band of H_3^+ at 200 and 20 K. The two strongest lines in the 200-K spectrum have intensities of 1.55 times the full scale of the figure, and the intensity scale of the 200-K spectrum is magnified by a factor of two relative to the 20-K spectrum.

extent of correlation than the matrix of correlation coefficients. It should also be noted that when three or more parameters are strongly correlated together, they have large κ_i values, although the correlation coefficients may not be close to ± 1. For example, three-parameter correlation matrices close to the singular matrix

$$\begin{bmatrix} 1 & -0.5 & -0.5 \\ -0.5 & 1 & -0.5 \\ -0.5 & -0.5 & 1 \end{bmatrix}$$

correspond to very strong correlations, although this is not apparent from the individual correlation coefficients. Experience with fits of other spectra suggests that the κ_i values in Table 3 are fairly typical, although some are larger than the largest found for the ND_4 spectrum (45).

Spectra at two different temperatures calculated from the constants of Table 3 are shown in Fig. 3. The 200-K spectrum is roughly typical of the laboratory experiments, whereas the 20-K spectrum is more appropriate for interstellar observations. Of the six lines that predominate at low temperatures, four (P^+, Q^+, R^-, and R^+) are from the lowest populated level (1, 1) and two (Q^- and R^+) are from the second lowest level (1, 0), which has a more favorable statistical weight factor. These six lines have all been measured and their wavenumbers are given in Table 1.

TABLE 4. Ground state rotational term values of H_3^+ (cm^{-1})*

J	K	$F_{obs.}(J,K)$	$F_{calc.}(J,K)$†	$F_{calc.}(J,K)$‡
1	0	86.963§	87.19	86.870
1	1	64.117§	64.30	64.048
2	1	237.351	238.04	237.093
2	2	169.272§	169.78	169.082
3	0	516.881	518.66	516.296
3	1	494.764	496.44	494.205
3	2	427.992	429.38	427.520
3	3	315.291§	316.30	314.927
4	1	833.566		832.596
4	2	768.441		767.564
4	3	658.655		657.923
4	4	501.940§		501.366

*Relative to the hypothetical $(J,K) = (0,0)$ level.
†Reference 15.
‡Reference 21.
§Calculated from the constants of Table 3. Other levels of the same K from observed differences.

In Tables 4 and 5, a set of 'experimental' term values for the ground and ν_2 state, respectively, are presented. These have been obtained by a least squares fit to the line wavenumbers, except that the lowest level of each K or G stack is calculated from the constants of Table 3. These tables should allow the best predictions at present of hitherto unobserved lines. Of special interest would be the forbidden transitions discussed by Aliev and Mikhailov (43), particularly the $\Delta K = \pm 3$ transitions in the ground state (46). Predictions of such $\Delta G = 3$ spectra depend at present on the scaled *ab initio* calculations, and therefore on the assumption that the correction factors for the *ab initio* B_0 and C_0 are equal. Observations of such transitions would, therefore, be of great interest. Figures 4 and 5 are energy-level diagrams for the rotational levels of the two states.

Possible perturbations affecting the levels (5, 2, ± 1) of the ν_2 state were mentioned above. The most likely candidate as a perturbing level is a level of the ν_1 state, and the lowest $J = 5$ level of ν_1 is the $K = 5$ level, which can perturb these levels through a $\Delta G = \pm 3$ perturbation. According to the calculated parameters of Carney and Porter (16), the rigid-rotor approximation would place the (5, 5) level of ν_1 a distance of 103 cm^{-1} above the (5, 2, 1) level of ν_2. The perturbation would be of the type $\Delta k = \pm 2$, $\Delta l_2 = \mp 1$, and the value of the matrix element calculated from the Carney and Porter parameters ($A_{nm} - B_{nm}$) or D_{nm} (16) is

TABLE 5. Rotational term values in the ν_2 state of H_3^+ (cm^{-1})*

		$F(J,G,-1)$		$F(J,G,1)$	
J	G	Observed†	Calculated‡	Observed†	Calculated‡
0	1		—	0	0
1	0	95.279	93.6		—
1	1		—	88.128	87.0
1	2		—	26.734	25.8
2	0		—	291.453	290.8
2	1	234.152	231.0	268.931	268.2
2	2		—	202.530	201.7
2	3		—	92.813	92.1
3	0	504.548	502.0		—
3	1	481.489	478.9	542.055	542.1
3	2	409.932	407.5	471.000	470.7
3	3		—	355.376	355.2
3	4		—	197.984	197.6
4	0		—	925.636	?
4	1	804.698	801.5	901.708	902.9
4	2	738.782	735.7	829.945	830.8
4	3	623.806	620.9	711.909	712.1
5	1	§		1341.981	
5	2	1138.914		1271.581	
5	3	1031.857		1152.487	
5	4	875.021		988.648	

*Relative to the $J = 0$ level at 2521.407 cm^{-1} (observed).
†Based on the observed lines and the term values of Table 4.
‡From ref. 21, averaged over degenerate pairs.
§Not observed.

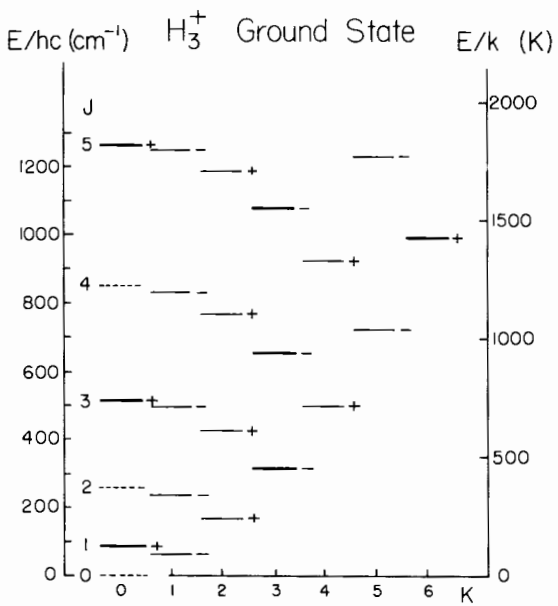

FIG. 4. Energy-level diagram for the ground vibrational state of H_3^+. Levels with $K = 0$ and even values of J (shown dashed) are forbidden by proton spin statistics. *Ortho*-levels (shown by bold lines) have a statistical weight of four and *para*-levels (shown by fine lines) have a statistical weight of two.

11 cm^{-1}. The resulting perturbation of $(11)^2/(103) = 1.2$ cm^{-1} will be shared between the two l-resonance levels (5, 2, ± 1).

This calculated perturbation is more than large enough to account for the observed residuals of these lines. However, the observed residuals are the differences from the positions predicted from the constants of Table 3, which must be effective constants that include the smaller effects of this perturbation on the other levels. Thus it will be necessary to examine the effects of the perturbation on the other levels before it can be regarded as definitely established. Observations of higher-J lines of the ν_2 band will also be of value, because the perturbation matrix elements increase with J, whereas the near-coincidences become closer for some of the higher-G levels.

5. Discussion

The present work is concerned with the observation and analysis of 46 lines of the ν_2 band of the H_3^+ ion. Of these lines, 44 have $J'' \leq 4$. This is a good fraction of the possible total of 54 allowed lines with $J'' \leq 4$. The Padé-type representations [3] and [6] have been very useful in fitting these observed lines, and a standard deviation of 0.014 cm^{-1} has been achieved in spite of the large size of the constants required for this very light

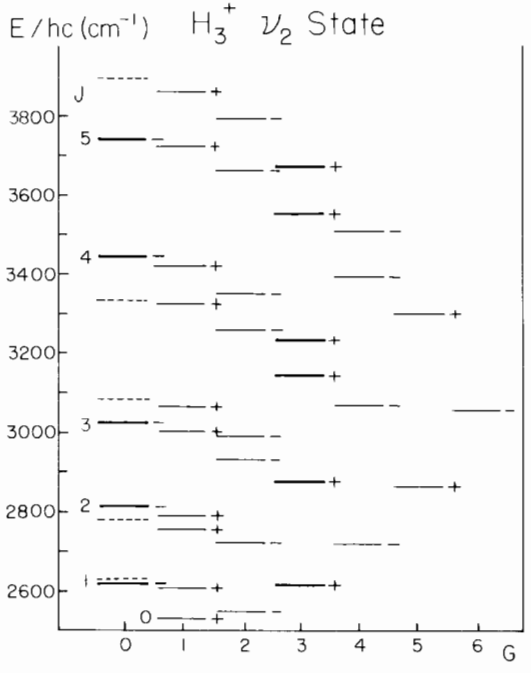

FIG. 5. Energy-level diagram for the ν_2 degenerate vibrational state of H_3^+. The quantum number G is equal to $|k - l_2|$. The statistical weights are represented as in Fig. 4.

molecule.

The observed spectrum corresponds closely to the *ab initio* predictions. A further implication of the *ab initio* matrix elements of Carney and Porter (16) is that perturbations between the rotational levels of the ν_2 and ν_1 states will become significant at higher J values, and there is evidence that such a perturbation is observed in the ν_2 (5, 2, ±1) levels. It will obviously be important to continue the observations to higher-J levels to establish this perturbation more definitely. More difficult will be the observation of transitions with $\Delta G \neq 0$, which will allow experimental values of C_ν, D_ν^{KK}, ... to be determined.

The observed spectrum lines can be used to monitor the presence, concentration, and rotational temperature of H_3^+. In the laboratory, such measurements will provide a valuable probe of conditions in hydrogenic discharges and other ion–molecule reaction systems. In space, the H_3^+ ion is of such great importance in theories of interstellar chemistry that the attempted observation (28) should be repeated with the object of either establishing the presence of this ion or reducing the present upper limit on its column density.

Acknowledgments

This paper is dedicated to Gerhard Herzberg on the occasion of his eightieth birthday. It is a pleasure to record his great inspiration and enthusiasm throughout this project. The ideas of the late Alex Douglas were of great importance in the original undertaking of this experiment. We are also grateful to Allen Karabonik and Trevor Sears for their assistance with the difference frequency and diode laser apparatuses, and to Walt Lafferty for precipitating the use of the Padé approximations. The research at the University of Chicago was supported by National Science Foundation grant PHY-8113097.

1. J. J. THOMSON. Philos. Mag. **24**, 209 (1912).
2. T. R. HOGNESS and E. G. LUNN. Phys. Rev. **26**, 44 (1925).
3. D. P. STEVENSON and D. O. SCHISSLER. J. Chem. Phys. **29**, 282 (1958).
4. H. EYRING, J. O. HIRSCHFELDER, and H. S. TAYLOR. J. Chem. Phys. **4**, 479 (1936).
5. A. J. DEMPSTER. Philos. Mag. **31**, 438 (1916).
6. M. YAMANE. J. Chem. Phys. **49**, 4624 (1968).
7. E. HERBST and W. KLEMPERER. Astrophys. J. **185**, 505 (1973).
8. W. D. WATSON. Rev. Mod. Phys. **48**, 513 (1976).
9. A. DALGARNO and J. H. BLACK. Rep. Prog. Phys. **39**, 573 (1976).
10. H. SUZUKI. Prog. Theor. Phys. **62**, 936 (1979).
11. S. S. PRASAD and W. T. HUNTRESS, JR. Astrophys. J. Suppl. Ser. **43**, 1 (1980); Astrophys. J. **239**, 151 (1980).
12. J. O. HIRSCHFELDER. J. Chem. Phys. **6**, 795 (1938).
13. G. D. CARNEY and R. N. PORTER. J. Chem. Phys. **65**, 3547 (1976).
14. G. D. CARNEY. Mol. Phys. **39**, 923 (1980).
15. G. D. CARNEY. Chem. Phys. **54**, 103 (1980).
16. G. D. CARNEY and R. N. PORTER. Phys. Rev. Lett. **45**, 537 (1980).
17. T. OKA. *In* Molecular ions: spectroscopy, structure and chemistry. *Edited by* T. A. Miller and V. E. Bondybey. North-Holland Publishing Co., Amsterdam, The Netherlands. 1983. pp. 73–90.
18. R. N. PORTER. Ber. Bunsenges. Phys. Chem. **86**, 407 (1982).
19. A. CARRINGTON and R. A. KENNEDY. J. Chem. Phys. **81**, 91 (1984).
20. P. G. BURTON, E. VON NAGY-FELSOBUKI, and G. DOHERTY. Chem. Phys. Lett. **104**, 323 (1984).
21. J. TENNYSON and B. T. SUTCLIFFE. Mol. Phys. **51**, 887 (1984).
22. T. AMANO and J. K. G. WATSON. J. Chem. Phys. **81**, 2869 (1984).
23. K. G. LUBIC and T. AMANO. Can. J. Phys. **62**, this issue.
24. G. HERZBERG. Trans. R. Soc. Can. **5**, 3 (1967).
25. T. OKA. Phys. Rev. Lett. **45**, 531 (1980).
26. R. C. WOODS. Rev. Sci. Instrum. **44**, 282 (1973).
27. A. S. PINE. J. Opt. Soc. Am. **64**, 1683 (1974); **66**, 97 (1976).
28. T. OKA. Phil. Trans. R. Soc. London Ser. A, **303**, 543 (1981).
29. G. HERZBERG. Trans. R. Soc. Can. **20**, 151 (1982).
30. T. AMANO. J. Chem. Phys. **79**, 3595 (1983).

31. C. S. GUDEMAN, M. H. BEGEMANN, J. PFAFF, and R. J. SAYKALLY. Phys. Rev. Lett. **50**, 727 (1983).
32. T. OKA. *In* Laser spectroscopy V. *Edited by* A. R. W. McKellar, T. Oka, and B. P. Stoicheff. Springer-Verlag, Berlin, Federal Republic of Germany. 1981. pp. 320–323.
33. T. A. DIXON and R. C. WOODS. Phys. Rev. Lett. **34**, 61 (1975).
34. D. J. NESBITT, H. PETEK, C. S. GUDEMAN, C. B. MOORE, and R. J. SAYKALLY. J. Chem. Phys. **81**, (1984).
35. F. C. VAN DEN HEUVEL and A. DYMANUS. Chem. Phys. Lett. **92**, 219 (1982).
36. S. C. FOSTER, A. R. W. MCKELLAR, and T. J. SEARS. J. Chem. Phys. **81**, 578 (1984); S. C. FOSTER and A. R. W. MCKELLAR. J. Chem. Phys. **81**, 3424 (1984).
37. I. DABROWSKI and G. HERZBERG. Acta Phys. Hung. In press.
38. J. K. G. WATSON. J. Mol. Spectrosc. **103**, 350 (1984).
39. S. P. BELOV, A. V. BURENIN, O. L. POLYANSKY, and S. M. SHAPIN. J. Mol. Spectrosc. **90**, 579 (1981).
40. A. V. BURENIN, O. L. POLYANSKII, and S. M. SHCHAPIN. Opt. Spectrosc. (Engl. Transl.), **53**, 395 (1982).
41. A. V. BURENIN, T. M. FEVRAL'SKIKH, E. N. KARYAKIN, O. L. POLYANSKY, and S. M. SHAPIN. J. Mol. Spectrosc. **100**, 182 (1983).
42. A. V. BURENIN, O. L. POLYANSKII, and S. M. SHCHAPIN. Opt. Spectrosc. (Engl. Transl.), **54**, 256 (1983).
43. M. R. ALIEV and V. M. MIKHAILOV. Acta Phys. Hung. In press.
44. J. K. G. WATSON. J. Mol. Spectrosc. **66**, 500 (1977).
45. F. ALBERTI, K. P. HUBER, and J. K. G. WATSON. J. Mol. Spectrosc. **107**, 133 (1984).
46. J. K. G. WATSON. J. Mol. Spectrosc. **40**, 536 (1971).